

# Optical Frequency Conversion Using a Linearized LiNbO<sub>3</sub> Modulator

Harold Roussel, *Member, IEEE*, and Roger Helkey, *Member, IEEE*

**Abstract**—High dynamic range optical frequency conversion is demonstrated using a third-order linearized modulator. A record dynamic range of 122.5 dB·Hz<sup>4/5</sup> was achieved at an input frequency of 400 MHz.

**Index Terms**—Frequency conversion, optical distortion, optical frequency conversion, optical mixing.

## I. INTRODUCTION

HIGH-LINEARITY optical links are needed for a variety of applications, from the distribution of cable TV signals [1] to antenna remoting [2]. The complexity of the receiver following the link can be reduced by including frequency conversion in the optical link [3]–[13], as the first frequency conversion stage is eliminated and an all-digital receiver may be possible because of the lower link output frequency. A frequency conversion radio frequency (RF) gain of 3.3 dB without an amplifier and a dynamic range of 112.9 dB·Hz<sup>2/3</sup> have been demonstrated using an unlinearized Mach–Zehnder modulator [13]. Frequency conversion using a third-order linearized electroabsorption modulator has given a dynamic range of 110 dB·Hz<sup>4/5</sup> [8].

For conventional suboctave links, the second-order intermodulation products fall out of band and third-order linearized modulators which do not suppress second-order distortion can be used. Third-order linearized modulators include the directional coupler [14], series-modulator [15], reflective half-coupler [16], and electroabsorption (EA) modulator [17], and are easier to fabricate and bias than modulators with second- and third-order linearization. In order to have second-order frequency products fall out of band for down conversion links, the output band after frequency conversion must be suboctave [8], resulting in a narrower frequency range than requiring the input band to be suboctave. Here, a dynamic range of 122.5 dB·Hz<sup>4/5</sup> is demonstrated using a half-coupler linearized modulator, which requires a suboctave output frequency band.

## II. EXPERIMENT

The experimental frequency conversion link configuration is shown in Fig. 1. The local oscillator signal is generated in a conventional quadrature-biased Mach–Zehnder modulator driven by a sinusoidal signal at the amplitude for minimum conversion loss [5], [8]. The input RF signal is applied to a linearized modulator. The linearized modulator used in

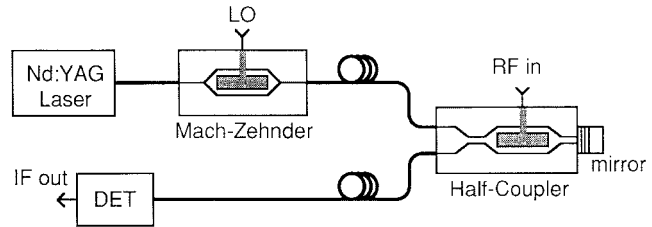


Fig. 1. Experimental configuration of high-linearity 400-MHz frequency conversion link using a conventional Mach–Zehnder modulator for the LO modulation and a reflective half-coupler Mach–Zehnder modulator for the RF signal.

this experiment is a reflective half-coupler Mach–Zehnder modulator from Uniphase Telecommunications Products, with an 18-mm lumped-element electrode. The linearized modulator bias point was set using a feedback circuit to provide a constant ratio between the input and output optical power [18].

The dc transfer function of a half-coupler modulator can be written as

$$I_d = \frac{I_m}{(1 - \beta)^2} \left( \cos^2 \left( \frac{\pi V}{2V_\pi} \right) - \beta \right)^2 \quad (1)$$

where

- $I_d$  photo detector current;
- $I_m$  maximum photo detector current;
- $V$  input voltage;
- $V_\pi$  half-wave voltage of the modulator;
- $\beta$  transfer function shape parameter that can be chosen by design.

The modulator used in this experiment had a  $\beta$  of 0.234. The half-coupler modulator can be designed to produce a variety of transfer functions corresponding to different  $\beta$  values as illustrated in Fig. 2. The circles indicate the bias points for minimum third-order distortion.

The secondary peak height of the half-coupler transfer function is determined by the coupling coefficients of the two directional couplers. These coefficients can be adjusted to set the height of the secondary peak and give maximum value of  $I_m$  set by the modulator insertion loss. The half-coupler modulator can be designed with a transfer function and noise figure that is identical to that of the third-order linearized series Mach–Zehnder configuration. The optimum value of  $\beta$  is determined by the noise figure tradeoff between reduced shot noise and reduced link gain at the linearized bias point [16].

The center of the half-coupler modulator electrode is offset from the mirror, so there is a time delay  $\tau$  between the modulation of the forward and reverse propagating optical waves which must be included in the model at higher frequency

Manuscript received April 28, 1998. This work was supported by the Department of the Air Force under Contract F19628-95-C-002.

The authors are with MIT Lincoln Laboratory, Lexington MA 02420 USA (e-mail: roussel@ll.mit.edu).

Publisher Item Identifier S 1051-8207(98)09513-0.

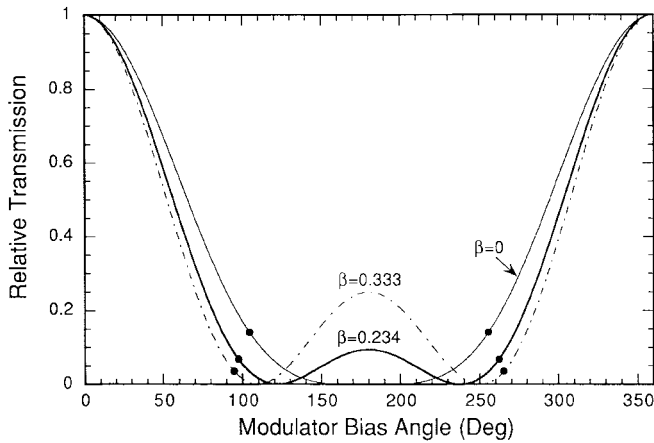


Fig. 2. Reflective half-coupler Mach-Zehnder modulator transfer functions for various values of the shape parameter  $\beta$ .

[16]. This delay can be explicitly included in the modulator transfer function using a model that treats the electrode as a lumped-element phase shift

$$I_d(t) = \frac{I_m}{(1-\beta)^2} \left( \cos^2 \left( \frac{\pi V(t)}{2V_\pi} \right) - \beta \right) \cdot \left( \cos^2 \left( \frac{\pi V(t+\tau)}{2V_\pi} \right) - \beta \right) \quad (2)$$

where  $V(t)$  is the time-dependent modulator voltage. This time dependence of the modulator transfer function results in some frequency dependence of the optimum bias point for linearization, which can be eliminated in the series modulator configuration by adding an electrical time delay before the second modulator electrode equal to the optical time delay.

The Mach-Zehnder modulator used to generate the local oscillator modulation had an input optical power of 364 mW, which gave an output optical power of 40.7 mW, resulting from 6.5 dB of optical insertion loss and 3 dB of loss due to quadrature modulator bias. There are more efficient methods to generate this optical modulation which could yield higher optical output power and better performance [13], such as optical amplification of the modulated signal [10], optical mode beating [19], or using a high-power laser modulated or pulsed at the local oscillator frequency.

The modulator was biased to cancel third-order distortion resulting in a measured spurious-free dynamic range of  $122.5 \text{ dB}\cdot\text{Hz}^{4/5}$  as shown in Fig. 3. The conventional spurious-free dynamic range definition was used, which is the input power range for a two-tone input signal where each of the fundamental tones are above the noise floor and each of the intermodulation products are below the noise floor [3], [20]. For a wide noise bandwidth, the dynamic range can be increased by biasing the modulator to give a finite amount of third-order distortion in order to cancel fifth-order distortion at a particular input power level [21]. By changing the modulator bias, the dynamic range in a 40-MHz bandwidth was increased from 60.4 to 64.7 dB as shown in Fig. 3, where the input power has been scaled slightly in the graph to account for the change in link gain due to the change in bias point.

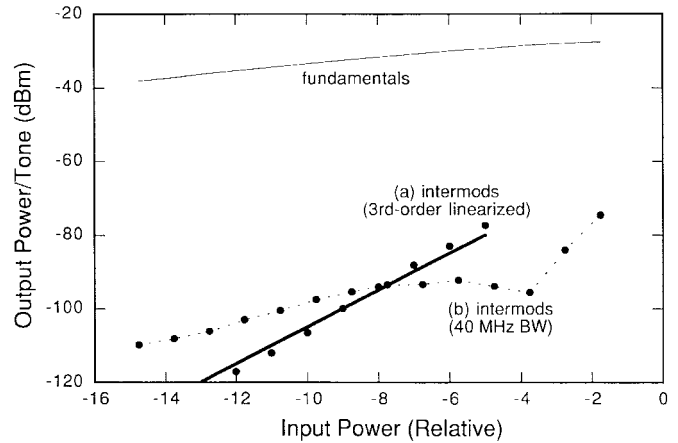


Fig. 3. Measured power levels of fundamental signals and intermodulation products as a function of input power level referenced to the modulator input for the linearized modulator frequency conversion link measured for  $f_{RF1} = 399 \text{ MHz}$ ,  $f_{RF2} = 401 \text{ MHz}$ ,  $f_{LO} = 420 \text{ MHz}$  for (a) third-order linearization (b) optimized for 40-MHz instantaneous bandwidth.

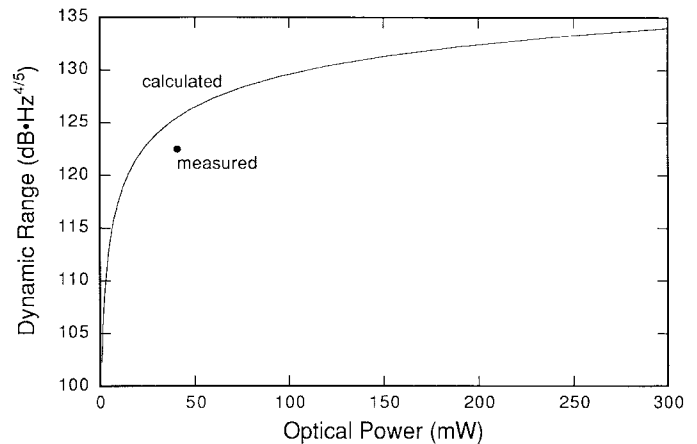


Fig. 4. Measured and calculated dynamic range as a function of optical input power to the linearized modulator for a modulator insertion loss of 6.5 dB and a detector efficiency of 0.88 mA/mW.

The measured dynamic range value is compared in Fig. 4 to calculations for a range of optical power using the transfer function model of (2). The measured dynamic range is approximately 3 dB lower than the modeled value, which may be due to using a lumped-element model for the modulator electrode. At higher frequency ( $>600 \text{ MHz}$ ) the calculated dynamic range degrades due to the delay between forward and backward propagating waves, and a different linearized modulator configuration should be used. This modulator was operated at the upper end of its bandwidth, and a traveling wave model has been shown to be important for accurately modeling distortion in linearized modulators without good match between the electrical and optical wave [22]. It is believed that these results could be improved using a different modulator electrode design.

### III. SUMMARY

A half-coupler linearized modulator has been used to demonstrate a record dynamic range for a linearized frequency conversion link. A dynamic range of  $122.5 \text{ dB}\cdot\text{Hz}^{4/5}$  was

achieved at 400 MHz, compared to previous frequency conversion link results of  $112.9 \text{ dB}\cdot\text{Hz}^{2/3}$  for a conventional Mach-Zehnder modulator and  $110 \text{ dB}\cdot\text{Hz}^{4/5}$  for a linearized electroabsorption modulator. The output frequency band must be suboctave to avoid second-order distortion products. This linearized modulator configuration should allow frequency conversion in links used for high-performance analog applications.

Link performance also has been calculated as a function of optical power and instantaneous bandwidth. The measured distortion was somewhat higher than predicted by a lumped-element model, and a traveling wave model may be needed at higher frequency. Using current technology, a dynamic range higher than  $134 \text{ dB}\cdot\text{Hz}^{4/5}$  should be possible for a frequency conversion link using an optimized laser and modulator.

#### ACKNOWLEDGMENT

The authors would like to thank E. Ackerman, G. Betts, M. Corcoran, C. Cox, D. Kettner, R. Knowlton, W. Song, M. Taylor, R. Taylor, and J. Twichell for their assistance and support.

#### REFERENCES

- [1] T. E. Darcie and G. E. Bodeep, "Lightwave subcarrier CATV transmission systems," *IEEE Trans. Microwave Theory Tech.*, vol. 38, pp. 524-533, 1990.
- [2] C. H. Cox, G. E. Betts, and L. M. Johnson, "An analytic and experimental comparison of direct and external modulation in analog fiber-optic links," *IEEE Trans. Microwave Theory Tech.*, vol. 38, pp. 501-509, 1990.
- [3] B. Kolner, "Electro-optic mixers," in *IEEE Topical Meeting on Optical Millimeter-Wave Interactions*, Newport Beach, CA, 1991, pp. 18-19.
- [4] G. K. Gopalakrishnan, W. K. Burns, and C. H. Bulmer, "Microwave-optical mixing in  $\text{LiNbO}_3$  modulators," *IEEE Trans. Microwave Theory Tech.*, vol. 41, pp. 2383-2391, 1993.
- [5] A. C. Lindsay, G. A. Knight, and S. T. Winnall, "Photonic mixers for wide bandwidth RF receiver applications," *IEEE Trans. Microwave Theory Tech.*, vol. 43, pp. 2311-2317, 1995.
- [6] D. Wake, C. R. Lima, and P. A. Davies, "Optical generation of millimeter-wave signals for fiber-radio systems using a dual semiconductor laser," *IEEE Trans. Microwave Theory Tech.*, vol. 43, pp. 2270-2276, 1995.
- [7] M. M. Howerton, R. P. Moeller, G. K. Gopalakrishnan, and W. K. Burns, "Low-biased fiber-optic link for microwave downconversion," *IEEE Photon. Technol. Lett.*, vol. 8, pp. 1692-1694, 1996.
- [8] C. K. Sun, R. J. Orazi, and S. A. Pappert, "Efficient microwave frequency conversion using photonic link signal mixing," *IEEE Photon. Technol. Lett.*, vol. 8, pp. 154-156, 1996.
- [9] C. K. Sun, R. J. Orazi, S. A. Pappert, and W. K. Burns, "A photonic-link millimeter-wave mixer using cascaded optical modulators and harmonic carrier generation," *IEEE Photon. Technol. Lett.*, vol. 8, pp. 1166-1168, 1996.
- [10] K. J. Williams and R. D. Esman, "Optically amplified downconverting link with shot-noise-limited performance," *IEEE Photon. Technol. Lett.*, vol. 8, pp. 148-150, 1996.
- [11] J. Önnegren and J. Svedin, "Photonic mixing using a Franz-Keldysh electroabsorption modulator monolithically integrated with a DFB laser," in *IEEE Int. Topical Meeting on Microwave Photonics*, Germany, 1996, Paper WE1-4.
- [12] K. P. Ho, S. K. Liaw, and C. Lin, "Efficient photonic mixer with frequency doubling," *IEEE Photon. Technol. Lett.*, vol. 9, pp. 511-513, 1997.
- [13] R. Helkey, J. Twichell, and C. Cox, "A down-conversion optical link with RF gain," *J. Lightwave Technol.*, vol. 15, pp. 956-961, 1997.
- [14] M. L. Farwell, Z. Q. Lin, E. Wooten, and W. S. C. Chang, "An electrooptic intensity modulator with improved linearity," *IEEE Photon. Technol. Lett.*, vol. 3, pp. 792-795, 1991.
- [15] G. E. Betts, "A linearized modulator for high performance bandpass optical analog links," in *IEEE MTT-S Int. Symp. Dig.*, 1994, pp. 1097-1100.
- [16] G. E. Betts, F. J. O'Donnell, K. G. Ray, D. K. Lewis, D. E. Bossi, K. Kissa, and G. W. Drake, "Reflective linearized modulator," *OSA Tech. Dig. Series: Integrated Photonics Research*, 1996.
- [17] R. B. Welstand, C. K. Sun, S. A. Pappert, Y. Z. Liu, J. M. Chen, J. T. Zhu, A. L. Kellner, and P. K. L. Yu, "Enhanced linear dynamic range property of Franz-Keldysh effect waveguide modulator," *IEEE Photon. Technol. Lett.*, vol. 7, pp. 751-753, 1995.
- [18] J. Schaffner and M. Hammond, U.S. Patent 5 488 503, 1996.
- [19] J. Czarske and H. Muller, "Heterodyne interferometer using a novel two frequency Nd:YAG laser," *Electron. Lett.*, vol. 30, pp. 970-971, 1994.
- [20] T. T. Ha, *Solid-State Microwave Amplifier Design*. Malabar, FL: Krieger, 1991.
- [21] A. Djupsjöbacka, "A linearization concept for integrated-optic modulators," *IEEE Photon. Technol. Lett.*, vol. 4, pp. 869-872, 1992.
- [22] U. V. Cummings and W. B. Bridges, "Bandwidth of linearized electrooptic modulators," *J. Lightwave Technol.*, vol. 16, pp. 1482-1490, Aug. 1998.